Steel and Composite Structures, *Vol. 33, No. 6* (*2019*) *823-836*
DOI: https://doi.org/10.12989/scs.2019.33.6.823

Push-out resistance of concrete-filled spiral-welded mild-steel and stainless-steel tubes

Chi K. Loke [1], Yasoja K.R. Gunawardena [1], Farhad Aslani*[1,2] and Brian Uy [3]

[1] *Materials and Structures Innovation Group*, *School of Engineering*, *The University of Western Australia*, *Crawley*, *WA 6009*, *Australia*
[2] *School of Engineering*, *Edith Cowan University*, *Joondalup*, *WA 6027*, *Australia*
[3] *School of Civil Engineering*, *The University of Sydney*, *Camperdown*, *NSW 2006*, *Australia*

(*Received August 20, 2019, Revised October 23, 2019, Accepted November 1, 2019*)

Abstract. Spiral welded tubes (SWTs) are fabricated by helically bending a steel plate and welding the resulting abutting edges. The cost-effectiveness of concrete-filled steel tube (CFST) columns can be enhanced by utilising such SWTs rather than the more conventional longitudinal seam welded tubes. Even though the steel-concrete interface bond strength of such concrete-filled spiral-welded steel tubes (CF-SWSTs) is an important consideration in relation to ensuring composite behaviour of such elements, especially at connections, it has not been investigated in detail to date. CF-SWSTs warrant separate consideration of their bond behaviour to CFSTs of other tube types due to the distinct weld seam geometry and fabrication induced surface imperfection patterns of SWTs. To address this research gap, axial push-out tests on forty CF-SWSTs were carried out where the effects of tube material, outside diameter (D), outside diameter to wall thickness (D/t), length of the steel-concrete interface (L) and concrete strength grade (f'_c) were investigated. D, D/t and L/D values in the range 102-305 mm, 51-152.5 and 1.8-5.9 were considered while two nominal concrete grades, 20 MPa and 50 MPa, were used for the tests. The test results showed that the push-out bond strengths of CF-SWSTs of both mild-steel and stainless-steel were either similar to or greater than those of comparable CFSTs of other tube types. The bond strengths obtained experimentally for the tested CF-SWSTs, irrespective of the tube material type, were found to be well predicted by the guidelines contained in AISC-360.

Keywords: bond strength; push-out tests; spiral-welded tubes; mild-steel; stainless-steel; analytical models

1. Introduction

Concrete-filled steel tubes (CFSTs) are a popular and widely used form of column construction. CFSTs utilising mild- and higher-carbon steel tubes have found applications in bridges, buildings and pile foundations over the years (Alfawakhiri 1997). The use of concrete-filled stainless-steel tubes (CFSSTs) has also been reported for structural columns located in durability critical environments (Tao *et al*. 2012). The cost-effectiveness of CFSTs could be improved through the use of spiral welding for fabricating the steel tube rather than conventional longitudinal seam welding. Spiral welded tubes (SWTs) are fabricated by helically bending a continuous coil of steel plate and welding together the abutting edges. The resulting spiral weld seam gives SWTs their name. The cost-benefits of such spiral welded tubes stem from the reduced capital costs of spiral tube mills (Knoop and Sommer 2004), increased efficiency due to the continuous nature of their fabrication (Kyriakides and Corona 2007) and since separate forming tools are not required for tubes of different diameters (Knoop and Sommer 2004). Especially in relation to larger diameter steel tubes, spiral welding provides a more economical fabrication method since SWTs of a range of different diameters can be formed from a given width of plate. In addition, in comparison to LWTs, SWTs offer longer joint-less lengths, speedier fabrication and smaller dimensional tolerances.

Even though previous studies which looked into the structural behaviour of concrete-filled spiral-welded steel tube (CF-SWST) columns have been reported in the literature, they were limited to considering member capacity behaviour (Gunawardena and Aslani 2018, 2019a, b, Gunawardena *et al*. 2019). The bond strength between the inside surface of the SWT and the concrete core was not evaluated explicitly in the afore-referenced studies. In practice, at connections between CFST and other CFST/non-CFST structural elements, it is common for the joint detail to only include fixities to the steel tube of the CFST (Zhang *et al*. 2012, Lyu and Han 2019). In such instances, and especially in the absence of any shear connectors, load transfer from the steel tube to the entire CFST section depends primarily on the bond between the steel tube and the concrete core. The non-provision of shear connectors is typically preferred to facilitate easier construction (Zhang *et al*. 2012, Tremayne *et al*. 2013). Hence, for practical applications of CF-SWST columns, it is necessary to establish characteristics of their ULS bond behaviour.

Push-out tests under concentric compressive loading are typically used to investigate the bond behaviour between the steel tube and concrete core of CFSTs. It is also generally accepted that the push-out bond behaviour of

*Corresponding author, Ph.D.,
E-mail: farhad.aslani@uwa.edu.au

ISSN: 1229-9367 (Print), 1598-6233 (Online)

CFSTs is governed by three contributing mechanisms, namely adhesion, mechanical interlocking and friction (Virdi and Dowling 1980, Roeder *et al*. 1999, Zhang *et al*. 2012, Chen *et al*. 2017, Fu *et al*. 2018, Guan *et al*. 2019, Lyu and Han 2019). Sadowski *et al*. (2015) reported that the spiral welding process causes unique surface imperfection patterns on the resulting steel tube. This, in turn, could potentially result in the interlocking bond behaviour of CF-SWSTs being distinct to that of CFSTs of other tube types. The interlocking may also be affected by the geometry of the spiral weld seam, which typically contains an inner weld bead as shown in Fig. 1. The inner bead of the spiral weld seam could potentially act as a shear connector as well, which may also result in the push-out behaviour of CF-SWSTs being different from that of CFSTs of other tube types. This is especially so since previous investigations have shown that the provision of mechanical connectors can have a beneficial effect on the bond behaviour of CFSTs (Shakir-Khalil 1993, Chen and Chen 2016, Tao *et al*. 2016). Given this context, it is clear that the ULS bond behaviour of CF-SWSTs warrants separate consideration.

Only one previous publication could be found in the literature which looked into the bond behaviour of CF-SWST columns (Tremayne *et al*. 2013, Lehman *et al*. 2018). This study, details of which can be found in Table 1, demonstrated that the ULS bond strength of carbon-steel CF-SWST columns can be significantly greater than those of equivalent CFSTs using LWTs. The results of Tremayne *et al*. (2013) indicate that the use of SWTs may also reduce the sensitivity of the bond behaviour to concrete shrinkage. However, only two CF-SWST specimens were tested in this study. No previous investigation could be found in the literature, which considered the push-out behaviour of concrete-filled spiral-welded stainless-steel tube (CF-SWSST) columns.

As listed in Table 1, several push-out investigations have been previously carried out on circular CFSTs of other non-SWT tube types. Consistent with the scope of this paper, only investigations which included purely axial push-out tests under monotonic loading conditions have been included in Table 1. In addition, previous push-out tests, which included the provision of additional shear connectors or special treatment of the steel-concrete interface have not been considered in this paper. Even though there exists no universal agreement, the results of previous investigations generally indicate that the bond strength decreases with increasing diameter (Roeder *et al*. 1999, Tao *et al*. 2016, Lyu and Han 2019), D/t ratio (Roeder *et al*. 1999, Chen *et al*. 2013, Ding *et al*. 2013, Fu *et al*. 2018, Lu *et al*. 2018a, b, Guan *et al*. 2019), and age (Virdi and Dowling 1980, Roeder *et al*. 1999, Abendeh *et al*. 2016, Tao *et al*. 2016). Furthermore, it is also generally accepted that concrete shrinkage has a detrimental effect on the bond strength of CFSTs (Roeder *et al*. 1999, Xu *et al*. 2009, Tremayne *et al*. 2013, Abendeh *et al*. 2016, Tao *et al*. 2016). On the other hand, the use of concrete types with expansive properties (Xu *et al*. 2009, Tao *et al*. 2016, Lu *et al*. 2018a, Yuan and Chen 2018), wet curing (Fu *et al*. 2018) and increased surface roughness (Fu *et al*. 2018) have been shown by several investigators to have a beneficial effect on the bond strength. It has been reported that any eccentricity of the applied axial load also increases the push-out bond strength of CFSTs (Roeder *et al*. 1999). However, the literature is less definitive on the effect of concrete compressive strength (f_{cm}) on bond strength. While some authors claim it has a positive effect (Yan *et al*. 2009, Chen *et al*. 2013, Lu *et al*. 2018a), a majority of investigators have concluded that its effect is either negligible (Virdi and Dowling 1980, Roeder *et al*. 1999, Morino and Tsuda 2003, Chen *et al*. 2017, Fu *et al*. 2018) or uncertain (Guan *et al*. 2019, Lyu and Han 2019). The effects of different concrete types, as well as interface length on the bond strength, have also not been conclusively established. Furthermore, in general, previous investigations have found that CFSSTs displayed reduced bond strengths compared to their mild- and higher-carbon steel counterparts (Tao *et al*. 2016).

It should be noted that several definitions of experimental push-out bond strength have been used in the literature, as can be seen from the details listed in Table 1. While the bond strength has generally been taken as that corresponding to the first peak of the load-slip curves when such a peak exists, identification of the ULS bond strength has been less unambiguous in the absence of such a peak. This was especially so where monotonically increasing load-slip curves were obtained experimentally (Virdi and Dowling 1980, Chen *et al*. 2017). The assumption of an average bond stress acting uniformly over the interface area between the steel tube and the concrete core, defined as per Eq. (1), has generally been used by previous investigators to quantify the bond strength. In Eq. (1), $P_{push\text{-}out}$ is the applied push-out load corresponding to the respective bond strength definition considered in the various test programs. The assumption of an ULS uniform bond stress has been justified by several previous investigators who measured approximately linear profiles of longitudinal strain along the length of the steel tubes of the respective CFSTs (Roeder *et al*. 2009, Grzeszykowski *et al*. 2017, Guan *et al*. 2019, Lyu and Han 2019).

$$\tau_{bond} = {P_{push-out}}\Big/{\pi(D-2t)L} \tag{1}$$

As noted in Table 2, a number of design standards (Architectural Institute of Japan (AIJ) 2001, European Committee for Standardization 2004, American Institute of Steel Construction 2016, Standards Australia 2017a, b) which provide guidelines for the design of carbon-steel CFST columns also specify design values for the ULS bond strength. Tao *et al*. (2016) found that the bond strengths obtained experimentally for the carbon-steel CFSTs they tested were greater than those specified by the respective standards (Standards Australia 2017). On the contrary, they found that the same standards could be non-conservative for CFSSTs.

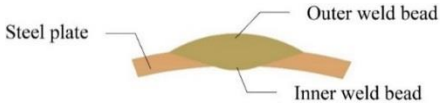

Fig. 1 Typical shape of spiral weld seam cross-section of SWTs (as seen at tube ends)

Table 1 Previously reported push-out test investigations on CF-SWSTs and circular CFSTs of other tube types

Reference	Steel tube type	Concrete type	D	D/t	$f_y/f_{0.2\%}$	f_{cm} (MPa)	τ_u definition	τ_u (MPa)
Lyu and Han (2019)	MS LWT	Normal/RAC	120, 200	30, 30.3	432.3, 392.4	31.7-38.8	Peak, inflexion point or at a bond strain of 0.0035	0.14-2.97
Guan *et al.* (2019)	MS LWT	Normal (using manufactured sand)	114	38, 32.6, 25.3	331, 302	51.8-101.4	Peak	2.34-4.29
Yuan and Chen (2018)	No data	Normal (with and without EAs)	165	55	Grade Q235	Grade C60	Peak	1.1-1.88
Lu *et al*. (2018b)	MS doubly LWTs	SFR-SCC with Eas	165	66, 47.1, 38.8	305.3-329.7	43.9, 44.4	Peak	0.63-2.92
Lu *et al*. (2018a)	MS doubly LWTs	SCC with and without SFs/EAs	165	66, 47.1, 38.8	305.3-329.7	No data	Peak	0.29-2.72
Fu *et al*. (2018)	MS LWT	LAC	114	28.5, 45.6	274.7, 305.6	23.7-30.2	Peak	1.25-2.50
Grzeszykowski *et al*. (2017)	No data	Normal	219.1	36.5	S235JR	47, 34.4	Peak	1.01, 0.84
Chen *et al*. (2017)	SS LWT	Normal	76	69.1-152	420	41.7, 26.6	Peak	0.068-0.243
Tao *et al*. (2016)	CS/SS LWTs	Normal with and without EAs, RAC	120, 400	30, 33.3, 50	321-372	42-81.8	Peak	0.04-1.85
Chen and Chen (2016)	No data	Normal	600	14	384	48.3	Peak	0.08
Abendeh *et al*. (2016)	No data	Normal/RuC	154.5, 107.7	28.7-26.8	308, 333	19.4	Peak	1.05-2.27
Xu *et al*. (2015)	MS LWT	Normal	114, 140, 165	28.5-36.7	312	32.6	Peak	1.27-1.65
Ke *et al*. (2015)	MS LWT	Normal (HSC)	110	36.7	398	57.2-64.4	Plateau	1.83-2.25
Tremayne *et al*. (2013), Lehman *et al*. (2018)	CS SWT/LWT	Normal (with and without LSA)	508	80	No data	54.8, 51.9	Peak / Max during test	0.04-0.84
Xu *et al*. (2013)	MS Seamless	Normal, RAC	140	46.7	345.9	31.6-49.2	Peak	1.16-1.94
Radhika and Baskar (2013)	Mild steel LWT	Normal with and without Metakaolin	150	30	319	43.1-57.2	Peak	1.78-2.43
Ding *et al*. (2013)	Seamless	SFR concrete with EAs	113, 127, 203	21.2, 25.4, 43.5	Q235/345	54.6-59.1	Peak	2.32-3.76
Yin and Lu (2010) Kang *et al.* (2010)	MS LWT	Normal	159	28.9, 35.3, 39.8	Q235	48.6	Plateau	0.80-1.52
Aly *et al.* (2010)	MS LWT	Normal	114	35.7	Grade350	32.5-57.5	Residual at large slip values	0.41-0.85
Yan *et al*. (2009)	Seamless	RPC	152	30.4	314	72.4, 61.6	Peak	0.59, 0.49
Xu *et al*. (2009)	No data	Normal with and without EAs	155.5-159	35.3-56.5	No data	37	Peak	0.60-0.67
Roeder *et al.* (1999)	No data	Normal with and without LSAs	274.5-609.6	20.4-109	No data	27.9-47.3	Peak	0.01-0.786
Shakir-Khalil (1993)	No data	Normal	168.3	48.1	No data	42, 44.3	Peak	0.65-0.93
Virdi and Dowling (1980)	MS Seamless	Normal	148.4-306	14.8-32.3	No data	22.0-46.3	At a bond strain of 0.0035	0.27-2.97

Table 2 Bond strengths specified in commonly used international design standards

Design standard	Specified bond strength (N/mm^2)
AS 2327 (2017)	0.55
AS 5100.6 (2017)	0.55
EC4 (2004)	0.55
AISC-360 (2016)	$5300\ t/D^2 \leq 1.4$
AIJ (2001)	0.15 (long term), 0.225 (short term)

Given this context, it is clear that for the application of CF-SWSTs as structural columns, the effects of the afore-mentioned pertinent parameters on their ULS bond behaviour need to be established. This paper discusses an experimental program which was carried out to address this identified research gap. The main aims of the experimental program were to obtain the push-out bond strengths effective for CF-SWSTs and to ascertain any differences in bond behaviour between CF-SWSTs and comparable CFSTs of other tube types. The applicability of the bond strengths specified in the relevant codified guidelines to CF-SWSTs was also evaluated as part of this study.

2. Experimental programme

In order to achieve afore-mentioned objectives, an experimental programme was formulated consisting of forty CF-SWST specimens, which included twenty CF-SWMSTs and twenty CF-SWSSTs. The main parameters that were varied were the tube material, outside diameter (D), wall thickness (t), length of the steel-concrete bond interface (L) and concrete strength grade (f'_c). The respective parameter values that were considered are given in Table 3. The geometries of the SWTs were chosen to cover a wide range of D/t values, including D/t values greater than 100. Even though D/t ratios in the region of 100 or above are used for actual engineering applications, especially in the United States (Roeder *et al*. 1999), previous push-out investigations have primarily been limited to specimens with much smaller D/t values. As can be seen from Table 1, only two previous investigations considered specimens with D/t values greater than 100.

2.1 Spiral-welded tubes

Mild-steel and austenitic stainless-steel SWTs, with nominal grades 250 and 316 respectively, were procured from a fabricator in New South Wales, Australia (ROLADUCT Spiral Tubing Group 2017). The weld seams of the SWTs were single-sided welds which had been welded from the outsides of the tubes. In order to determine the in-situ material strengths of the SWTs tensile tests were conducted on representative steel coupons as per AS 1391 (Standards Australia 2007). For the mild-steel SWTs coupons were extracted from a representative length of virgin plate while for the stainless-steel SWTs coupons were extracted from a SWT in its welded state as well as from a length of virgin plate. The material strength

Table 3 Parameters considered for the test programme

Parameter	Values considered
SWT material	Mild-steel (M), Stainless-steel (S)
Tube outside diameter (D) - D1, D2, D3 (mm)	102, 203, 305
Tube wall thickness (mm)	2, 3
Bond interface length – L1, L2	3D-125, 6D-125
Nominal concrete strength grade (f'_c) – A, B	20, 50

Table 4 Steel material properties obtained from coupon tests

Coupons cut from virgin plate				Coupons cut from SWT in its welded state	
Mild-steel		Stainless-steel		Stainless-steel	
f_y (MPa)	234.9	$f_{0.2\%}$ (MPa)	271.7	$f_{0.2\%}$ (MPa)	262.5
E_s (GPa)	200	E_0 (GPa)	191	E_0 (GPa)	187
		n	7.69	n	7.5

parameters obtained from the coupon tests are given in Table 4. The parameters listed in Table 4 for stainless-steel are those corresponding to the material model proposed by Rasmussen (2003), which were calculated using the experimentally obtained data. In Table 4, f_y and E_s denote the yield strength and elastic modulus of mild-steel, while $f_{0.2\%}$, E_0 and n represent the 0.2% proof-strength, initial modulus and non-linearity coefficient of stainless-steel as defined in Rasmussen (2003). The stress-strain curves obtained experimentally from the coupons tests, corresponding to the values listed in Table 4, can be found in Gunawardena and Aslani (2018, 2019a).

2.2 Specimen preparation and concrete material properties

Ready-mix self-compacting concrete of nominal grades 20 MPa and 50 MPa was used for infilling the SWTs. The maximum aggregate sizes of the concrete mixes were 10 mm and 14 mm for the 20 MPa and 50 MPa grades respectively. All the SWTs which were to be filled with the same grade of concrete were infilled using a single batch of the respective concrete mix. Slump flow values of 534 mm and 530 mm were obtained on-site for the 20 MPa and 50 MPa concrete mixes respectively. Prior to filling the SWTs with concrete, 25 mm thick circular shaped wooden plugs were fixed to one end of the tubes. The SWTs were then stood up vertically on a level surface so that the wooden plugs were at the bottom, in preparation for concrete pouring. Concrete was poured into the specimens until the gap between the top of each SWT and the as-cast level was approximately equal to 100 mm. This gap was left in order to enable movement of the concrete core during the subsequent push-out tests. The specimens were thereafter cured for 28 days using ponded water on the as-cast surface

Table 5 Results obtained from concrete cylinder compression tests and definitions of strength gain curves

Nominal Grade 20 MPa			Nominal Grade 50 MPa		
No. of days after casting (t_{age})	Mean	Stdev	No. of days after casting (t_{age})	Mean	Stdev
7	23.3	1.2	7	28.0	1.6
28	26.8	3.4	90	57.2	0.5
56	27.3	5.6			
Definition of strength gain curve	$f_{cm} = 2.030 \ln(t_{age}) + 19.498$ (MPa)		$f_{cm} = 11.417 \ln(t_{age}) + 5.831$ (MPa)		

of the concrete.100 mm diameter and 200 mm high concrete cylinders were also cast at the time of the respective concrete pours.

The concrete compressive strength at the time of testing (f_{cm}) corresponding to each test specimen was calculated using strength gain curves, as defined in Table 5. These strength gain curves were approximated using the results obtained from concrete cylinder compression tests which were conducted throughout the experimental program. Results of these compression tests are tabulated in Table 5. f_{cm} values corresponding to each test specimen are listed in Table 6. In Table 6 as well as in this paper in general, each test specimen is represented by a label of the form 'MSD1L12A' which contains the steel material type (mild steel (MS), stainless-steel (SS)), outside tube diameter (D1-3), interface length (L1-2), wall thickness (2, 3 mm) and concrete grade (20MPa - A / 50 MPa - B).

2.3 Experimental setup

The test setup that was used for the push-out tests is shown schematically in Fig. 2. For the push-out tests, the CF-SWST specimens were inverted from their as-cast

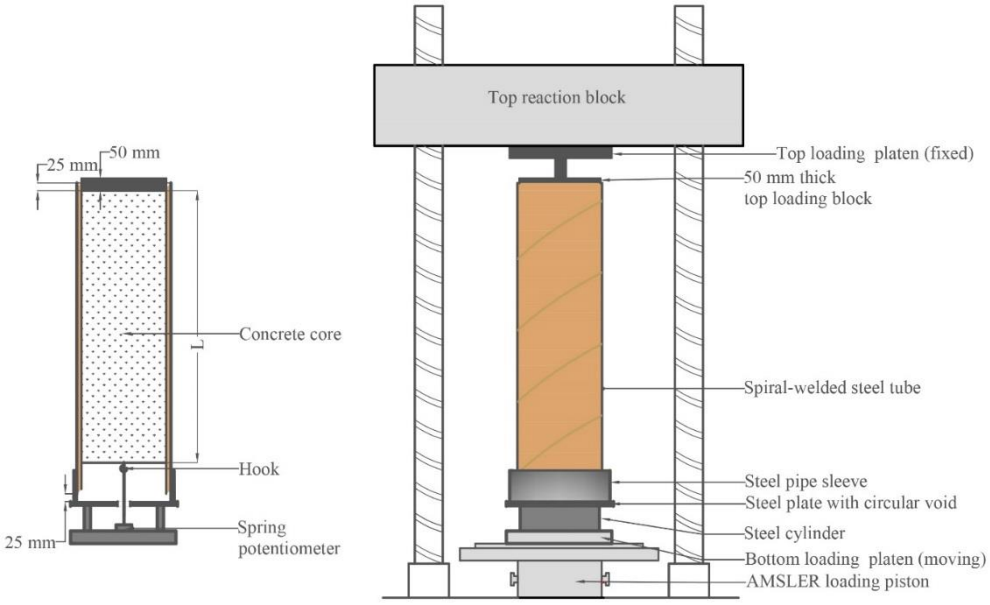

(a)

(b)

(c)

Fig. 2 (a) Schematics of loading setup used for the CF-SWST push-out tests; (b) and (c) images of actual setups of specimens MSD2L12A and SSD1L22A

vertical orientation. In order to ensure that local buckling did not occur within the 100 mm length of tube which was not filled with concrete, the hollow end of the respective specimens was stiffened by structurally welding on a steel pipe sleeve, as shown in Fig. 2. For the test setup, initially, a spring potentiometer was magnetically attached to the centre of the bottom loading platen of the AMSLER testing machine that was used for the testing. A high strength thick circular steel ring was then placed on the loading platen upon which a steel plate with a circular opening was subsequently placed. This allowed the cable of the spring potentiometer to be attached to a hook fixed to the bottom of the concrete core of the test specimen. The respective test specimen (after welding on the steel pipe sleeve) was thereafter placed vertically on the afore-mentioned steel plate and positioned so that the axis of the CF-SWT was coincident with the loading axis of the machine. A 50 mm thick circular steel plate, with a diameter slightly smaller than the inner diameter of the SWT, was used to ensure that only the concrete core was loaded at the top end. At the bottom end of the test specimen, the load from the testing machine was transferred on to the steel pipe sleeve, which in turn transferred it to the steel section of the CF-SWST. The spring potentiometer effectively measured the movement of the loading platen relative to the bottom of the concrete core of the respective CF-SWST. Even though this measurement also includes any compression that would have occurred in the concrete core, steel tube and pipe sleeve, those contributions would have been much smaller compared to the contribution of the relative slip between the core and the SWT (Lyu and Han 2019). Therefore, the measurement from the spring potentiometer has been taken to be equal to the interface slip (s) in this paper. In addition to the slip, the applied load (P) was also measured through a load-cell in-built with the testing machine. Displacement control loading was used for the testing. The loading rate was kept below 1 mm/min to ensure quasi-static loading. The loading rate that was used for the tests compares well with those reported in the literature where displacement control loading rates of 0.762, 1, 0.6, 1.2, 0.3 and 0.25 were reported by Tremayne *et al*. (2013), Lyu and Han (2019), Guan *et al*. (2019), Yuan and Chen (2018), Tao *et al*. (2016) and Aly *et al*. (2010). In general, the loading was continued until a slip in the region of 40 mm was achieved. As can be seen from Table 6, at the time of testing the concrete age of the respective CF-SWSTs ranged from 35 to 58 day. It should be noted that no visually distinguishable gap between the SWT and the concrete core, attributable to the shrinkage of concrete, was observed at the time of testing for any of the specimens.

3. Results and discussion

3.1 Failure modes and load-slip behaviour

The load-slip data obtained from the push-out tests are plotted in Fig. 3. For the plots shown in Fig. 3, the measured loads were converted to average bond stress values (τ) by dividing them by the respective interface areas following the definition stated in Eq. (1). As discussed

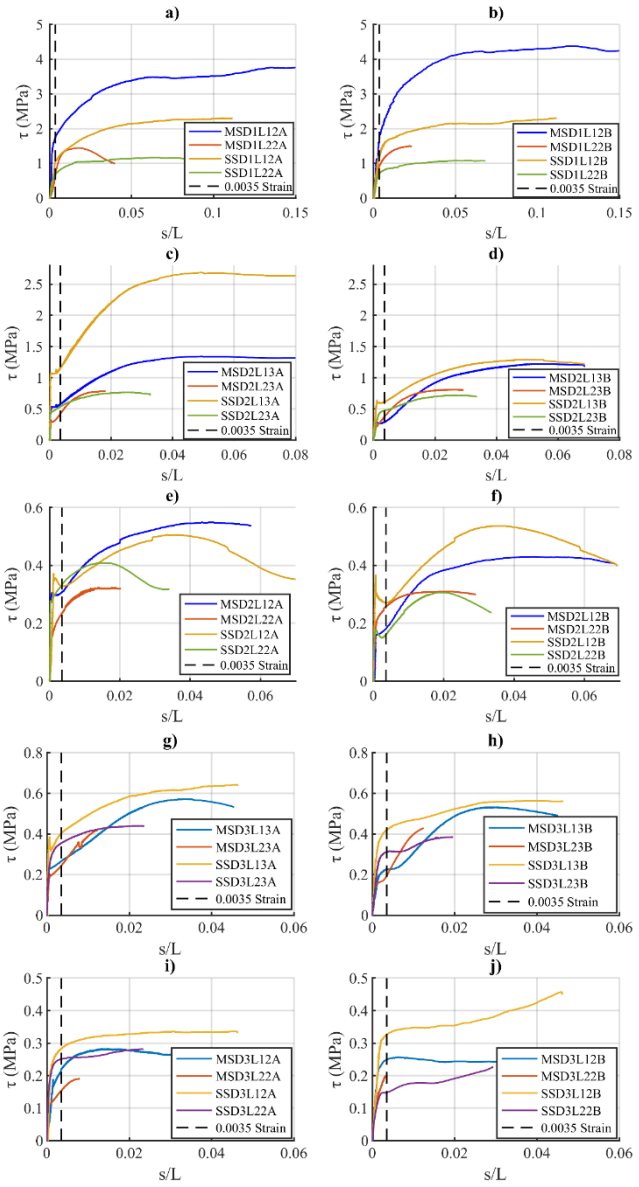

Fig. 3 τ-ε_{bond} plots obtained for the tested CF-SWMSTs and CF-SWSSTs containing (a), (c) and (e) Grade 20 MPa concrete with D/t equal to 51, 67.7 and 101.5; (b), (d) and (f) Grade 50 MPa concrete with D/t equal to 51, 67.7 and 101.5; (g) and (i) Grade 20 MPa concrete with D/t equal to 101.7 & 152.5; (h) and (j) Grade 50 MPa concrete with D/t equal to 101.7 & 152.5

previously, this is consistent with the typical approach that has previously been used to quantify the push-out bond strength. In Fig. 3, the measured slip (s) has also been normalised by the respective interface length. The ratio of interface slip to interface length (s/L) has been termed 'bond strain (ε_{bond})' by previous researchers who also used a limiting bond strain criterion to define the ultimate limit state bond strength (Virdi and Dowling 1980, Tao *et al*. 2016, Lyu and Han 2019).

As can be seen from Fig. 3, in general, the τ-ε_{bond} plots obtained for the tested CF-SWSTs displayed similar behaviour irrespective of the tube material or interface

length. Typically, the τ-ε_{bond} plots consisted of an initial linear portion which was limited to extremely small values of slip and was followed by a non-linear region. In this non-linear region, for a majority of the tested specimens, the load-slip curve increased monotonically but with a reducing rate of increase until large magnitudes of slip. This behaviour is consistent with that reported previously by Tremayne *et al*. (2013) for the carbon-steel CF-SWSTs they tested. At large values of slip, it was observed that the respective plots either contained a peak or plateaued out. For a few of the tested specimens, the τ-ε_{bond} plots also contained a local peak which occurred after a brief non-linear portion that followed the initial linear segment of the respective plots. The bond stress (and hence the push-out load) was observed to drop sharply at these local peak locations after which it again increased as described previously. It is the authors' opinion that these local peaks may have occurred as a result of the variability of the thickness of the inner bead of the weld seam of the tested SWTs. As has been established previously, monotonically increasing load-slip plots result when the push-out resistance due to micro-interlocking is less than that due to the combined effects of macro-interlocking and friction (Chen *et al*. 2017, Lyu and Han 2019). The provision of mechanical connectors along the tube inside surface of a CFST can result in such a condition (Tao *et al*. 2016). A majority of the τ-ε_{bond} curves obtained from the CF-SWST push-out tests was similar to the corresponding behaviour obtained by Tao *et al*. (2016) for a CFST with inner steel rings. Therefore, it can be rationally thought that the inner bead of the SWT also acts as an internal mechanical connector. However, if the weld bead thickness is small, the behaviour may revert to that of a typical CFST, which overwhelmingly displays a peak push-out load as can be seen from the data in Table 1. It should be noted that such local peaks would be unlikely for double-sided SWTs, such as those tested by Tremayne *et al*. (2013), as double-sided welding results in much larger inner bead thicknesses. For example, an inner bead thickness of 3 mm was reported by Tremayne *et al*. (2013).

Given that a majority of the τ-ε_{bond} plots did not contain a peak at smaller values of slip, the experimental ULS bond strength (τ_u) was adopted as the bond stress corresponding to a bond strain (i.e., s/L) of 0.0035 as per the definition proposed by Virdi and Dowling (1980). This definition is qualitatively based on the premise that the ULS bond failure is associated with localised concrete crushing in the micro-interlocked regions. Tao *et al*. (2016) and Lyu and Han (2019) also used this definition of bond strength for specimens which did not display a clear peak in the respective load-slip plots. The peaks and plateaus which were obtained at larger values of slip for the tested specimens were not considered for τ_u as such levels of slip were judged to be non-conservative for structural applications. The bond strengths obtained in this manner are given in Table 6.

At the point of termination of the respective push-out tests, an accumulation of crushed concrete together with a continuous circumferential gap was observed at the top ends of the specimens, as shown typically in Fig. 4. This was the

Table 6 Experimental details of test specimens and experimentally obtained bond strengths

Specimen label	D	t	D/t	L/D	CF-SWMSTs						CF-SWSSTs					
					Grade 20 MPa			Grade 50 MPa			Grade 20 MPa			Grade 50 MPa		
					t_{age} (days)	f_{cm} (MPa)	τ_u (MPa)	t_{age} (days)	f_{cm} (MPa)	τ_u (MPa)	t_{age} (days)	f_{cm} (MPa)	τ_u (MPa)	t_{age} (days)	f_{cm} (MPa)	τ_u (MPa)
MSD1L12A/B, SSD1L12A/B	102	2	51.0	1.8	40	27.0	1.75	50	50.5	1.70	35	26.7	1.05	50	50.5	1.18
MSD2L12A/B, SSD2L12A/B	203	2	101.5	2.9	44	27.2	0.31	48	50.0	0.18	43	27.1	0.33	48	50.0	0.27
MSD3L12A/B, SSD3L12A/B	305	2	152.5	2.9	41	27.0	0.15	42	48.5	0.25	51	27.5	0.28	42	48.5	0.33
MSD2L13A/B, SSD2L13A/B	203	3	67.7	2.9	50	27.4	0.58	49	50.3	0.29	42	27.1	1.16	49	50.3	0.61
MSD3L13A/B, SSD3L13A/B	305	3	101.7	2.9	51	27.5	0.27	42	48.5	0.23	50	27.4	0.40	42	48.5	0.42
MSD1L22A/B, SSD1L22A/B	102	2	51.0	5.8	40	27.0	0.64	51	50.7	0.91	41	27.0	0.67	50	50.5	0.70
MSD2L22A/B, SSD2L22A/B	203	2	101.5	5.9	48	27.4	0.24	44	49.0	0.26	44	27.2	0.33	43	48.8	0.16
MSD3L22A/B, SSD3L22A/B	305	2	152.5	5.9	49	27.4	0.41	44	49.0	0.20	57	27.7	0.25	37	47.1	0.15
MSD2L23A/B, SSD2L23A/B	203	3	67.7	5.9	58	27.7	0.22	41	48.2	0.37	48	27.4	0.54	43	48.8	0.47
MSD3L23A/B, SSD3L23A/B	305	3	101.7	5.9	56	27.7	0.25	41	48.2	0.19	55	27.6	0.36	40	47.9	0.31

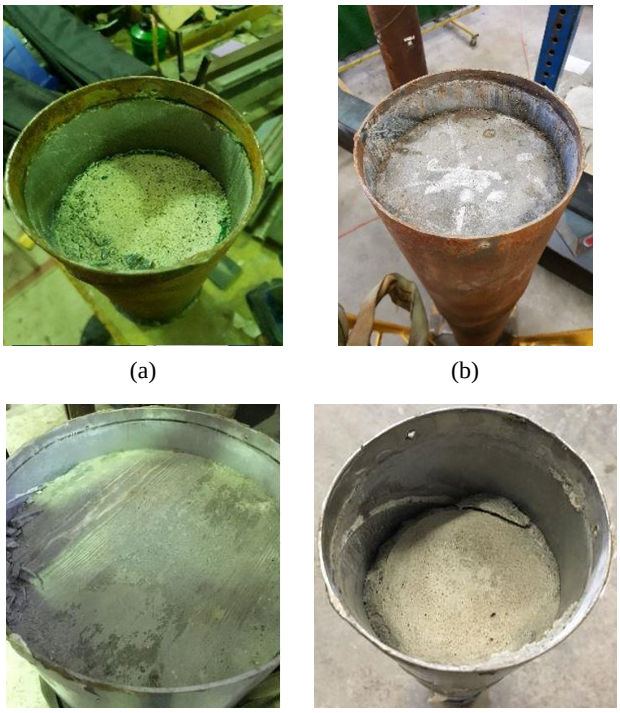

(a) (b)

(c) (d)

Fig. 4 Condition of the top end of the tested specimens at point of test termination (a) MSD1L12A; (b) MSD2L23; (c) SSD3L12B; d) SSD1L22A

case for both mild-steel as well as stainless-steel CF-SWSTs irrespective of the interface length considered. After the tests, the respective SWTs were cut and removed to investigate the states of the outside surfaces of the respective concrete cores. As shown typically in Fig. 5, all the specimens displayed scratch marks with an extent equal to the total slip that was achieved during the respective tests. Some local crushing of the concrete was also observed for the specimens where the inner weld bead had keyed into the concrete during slippage. However, the depth of keying and extent scratching were not consistent, which indicated the variability of the inner weld bead thickness.

3.2 Variation of bond strengths with pertinent parameters

The variations of the bond strength obtained for the tested CF-SWMSTs and CF-SWSSTs with the respective D/t, D and L/D values are plotted in Figs. 6, 7, and 8 respectively. For comparison, the bond strengths previously reported in the literature for non-SWT CFSTs with comparable concrete strengths are also plotted in Figs. 6-7. Out of the tests listed in Table 1, only those which had been carried out at concrete ages less than 120 days were considered for comparison. In addition, previously tested CFSTs for which expansive agents had been used in the respective concrete mixes were also not considered for Figs. 6 and 7. For a rational comparison with the tested CF-SWSTs, which had nominal concrete grades 20 MPa and 50 MPa, the previous test results were separated into two groups, namely, those which had test day strengths from 20

(a)

(b)

(c)

(d)

Fig. 5 Condition of the steel-concrete interface at point of test termination - (left to right) concrete core, spiral weld and inside surface of steel tube for (a) MSD2L12A; (b) MSD2L23B; (c) SSD3L12A; and (d) SSD3L23B

– 40 MPa and 40–60 MPa respectively. In Fig. 8, the bond strengths reported by Virdi and Dowling (1980), Shakir-Khalil (1993), Yin and Lu (2010) and Radhika and Baskar (2012) for mild-steel CFSTs and by Chen *et al*. (2017) for CFSSTs are plotted for comparison. In these test programmes, the only variable parameter that was

considered was the interface length. On average, it was found that that bond strengths obtained for mild-steel and stainless-steel CF-SWSTs were largely comparable in magnitude. On the contrary, for CFSTs of other non-SWT tube types, it has been reported that the bond strength reduces when stainless-steel tubes are used compared to their mild- or carbon-steel counterparts (Tao *et al*. 2016, Chen *et al*. 2017). It is possible that the similarity of bond strengths between mild-steel and stainless-steel CF-SWSTs results from the contribution of the inner weld bead to the mechanism of push-out resistance.

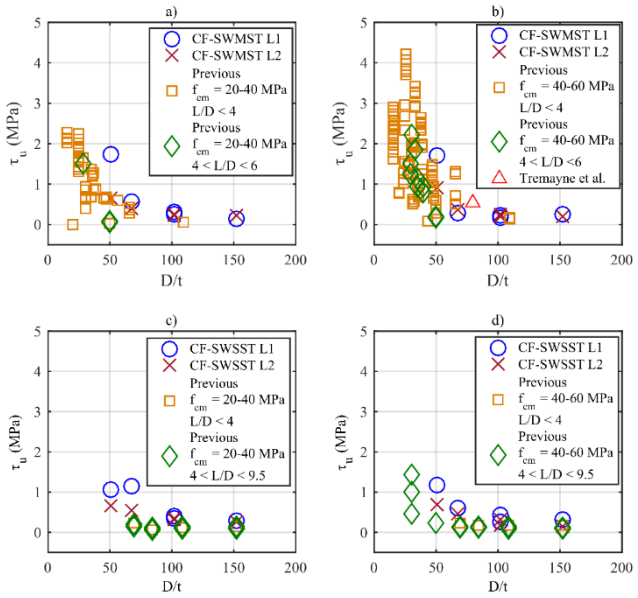

Fig. 6 Variation of bond strength with D/t for the tested (a), (b) CF-SWMSTs with Grade 20 MPa and 50 MPa concrete respectively; and (c), (d) CF-SWSSTs with Grade 20 MPa and 50 MPa concrete respectively

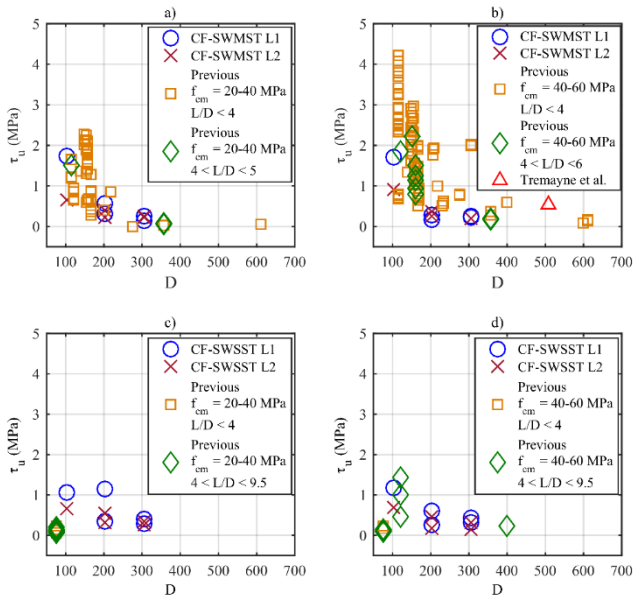

Fig. 7 Variation of bond strength with outside tube diameter (D) for the tested (a), (b) CF-SWMSTs with Grade 20 MPa and 50 MPa concrete respectively; and (c), (d) CF-SWSSTs with Grade 20 MPa and 50 MPa concrete respectively

As can be seen from Figs. 6-7, it was observed that the variations of τ_u with D/t and D were similar to those reported previously for CFSTs of other tube types. The bond strengths obtained for the CF-SWMSTs were greater than those of mild-steel CFSTs of other tube types for smaller D/t values and became more comparable for larger values of D/t. On the contrary, the tested CF-SWSSTs displayed consistently greater bond strengths than those reported for CFSSTs of other tube types, over the full range of the tested D/t values. These results indicate that the bond strengths of CF-SWSTs, irrespective of the tube material, are similar to or more superior than those of CFSTs of other tube types. Taken together with the results of previous investigations (Gunawardena and Aslani 2018, 2019a,b, Gunawardena *et al*. 2019), this provides further evidence that SWTs can be used for CFSTs as direct replacements for other tube types.

It was observed that for the tested CF-SWST specimens, the bond strength decreased significantly as the D/t ratio increased. This suggests that the existence of the inner weld seam was possibly not fully adequate to negate the detrimental effects of shrinkage, which occurs for larger diameter specimens, as discussed by Roeder *et al*. (1999). It is possible that for CFSTs using SWTs with double-sided welds, which would have inner weld beads with greater thickness than the tubes considered in this paper, the reduction of bond strength with D/t would be less. This postulation needs to be verified through further investigation.

As is evident from Fig. 8, no clear trend could be identified for the bond strength with purely the L/D ratio. For reference, the bond stresses corresponding to a bond strain of 0.0035 for the two CF-SWMSTs tested by Tremayne *et al*. (2013) are also shown in Figs. 6(b) and 7(b). These tests had concrete strengths (f_{cm}) equal to 51.9 and 54.8 MPa respectively. The bond stresses were obtained from the respective load-slip curves that were reported. As can be seen from Figs. 6(b) and 7(b), the bond stresses obtained by Tremayne *et al*. (2013) were observed to be

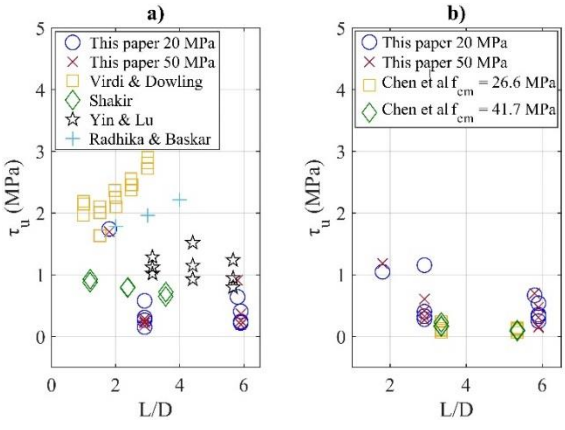

Fig. 8 Variation of bond strength with L/D for the tested: (a) CF-SWMSTs; and (b) CF-SWSSTs

greater than the corresponding values indicated by the experimentally obtained trends of τ_u with D and D/t for the tested CF-SWMSTs. This mismatch could possibly be explained by the fact that Tremayne *et al*. (2013) used SWTs with double-sided welds. Such SWTs can be expected to contain inner weld beads of larger thickness than those that would have been present in the SWTs described in this paper, for which the weld seams were all single-sided welds. An inner bead of greater thickness would result in enhanced mechanical interlock and as a consequence display a higher bond strength. Nonetheless, this assertion needs to be verified through further tests of comparable SWTs with double and single sided weld seams.

However, it was observed that for a given tube geometry (i.e., D/t ratio) and concrete strength the specimens with the higher L/D ratio displayed a slightly reduced τ_u. While this was the case for a majority of the tube geometries, a few displayed the opposite behaviour as well. The reduction of bond strength with L/D could be due to an inadequacy of the assumption of constant bond stress over the interface area for the specimens with longer interface lengths. For the longer specimens, it is possible that the bond transfer length was less than the total interface length. If that was indeed the case, the bond strengths calculated as per Eq. (1) would be underestimates. A reducing trend of τ_u with L/D was also reported by Fu *et al*. (2018) who considered L/Ds in the range 3.1 to 6.8.

Further investigation is required to establish whether the observed reduction in bond strength with L/D was indeed caused due to the reasons discussed above. Push-out tests, where the outside surface of the SWT is instrumented with several closely spaced strain gauges along its height would be useful for this purpose. Through such tests, it would be possible to determine how the push-out load is transferred along the length of the specimen, which can then be used to ascertain the bond transfer length.

No consistent trend could be observed for the bond strength with f_{cm} for the tested CF-SWSTs. However, on average, it could be observed that increasing f_{cm} (i.e., increasing concrete grade) results in a decrease in the bond strength, albeit with significant scatter.

4. Methods and predicting interface bond strength of CF-SWSTs

4.1 Bond strengths specified by codes of practice

In Fig. 9, the experimentally obtained bond strengths are compared to those predicted by five internationally used CFST design standards, namely Standards Australia (2017a, b), European Committee of Standardization (2004) (EC4), American Institute of Steel Construction (2016) and AIJ (2001).

It can be seen that for both mild-steel and stainless-steel CF-SWSTs, the guidelines of AISC-360 give conservative predictions of bond strength which are also in good agreement with the experimentally obtained values. The agreement is especially close for smaller values of t/D2, corresponding to larger diameters and larger D/t ratios. The

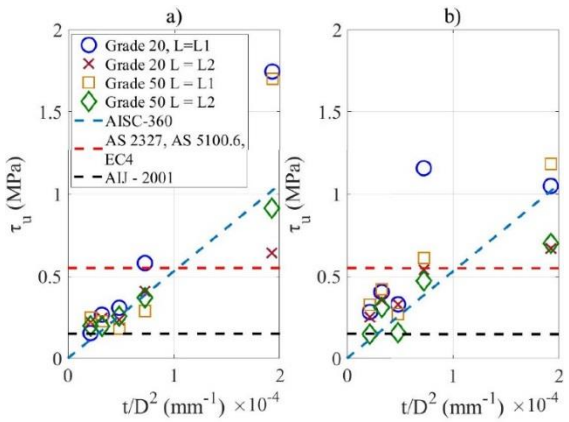

Fig. 9 Comparison of bond strengths obtained for the tested CF-SWSTs with those specified by various codified guidelines, of (a) CF-SWMSTs; and (b) CF-SWSSTs

conservativeness of the predictions increases with t/D2, particularly for CF-SWMSTs.

However, it can also be seen from Fig. 9 that for the longer specimens of the smallest diameter that was tested (i.e., with the largest t/D^2 ratio) the predictions of AISC-360 are non-conservative. As discussed earlier, this may be related to the fact that the assumption used to calculate τ_u could have resulted in the bond strengths being under-estimated for the specimens with the longer interface lengths.

It was also observed that the bond strength value of 0.55 MPa specified by AS 2327, AS5100.6 and EC4 is, in general, non-conservative for CF-SWMSTs and CF-SWSSTs. This was the case except for specimens with low values of diameter and D/t ratio. On the other hand, the bond strength specified in AIJ, equal to 0.15 MPa, provided a good lower bound of the bond strengths obtained experimentally for the tested CF-SWSTs. However, the conservativeness of this bond strength value was excessive for specimens with smaller values of D/t.

4.2 Predictive equations proposed by previous investigators

In addition to the guidelines provided in various codes of practice, a number of previous investigators have also proposed predictive models for the bond strength of CFSTs. The bond strengths predicted by four such proposed models, given in Eqs. (2)-(5), were calculated for the tested CF-SWSTs for comparison with the experimental values. The corresponding actual-to-predicted bond strength ratios ($\tau_{u\_experimental}/\tau_{u\_predicted}$) are given in Table 7. For this comparison, only the specimens with the shorter interface length (i.e., L_1) were considered since the bond strengths calculated for the longer specimens may be under-estimates, as discussed previously. Eqs. (2) to (5) were proposed by Lyu and Han (2019), Zhang *et al*. (2012), Lu *et al*. (2018a) and Roeder *et al*. (1999) respectively. For t and D in Eqs. (2)-(5) the respective magnitude in mm should be used. On average, it was observed that except for the model proposed by Lyu and Han (2019), the bond strengths obtained

Table 7 Comparison of predicted bond strengths with those obtained experimentally for the tested CF-SWSTs

Specimen label	$\tau_{u\_experimental}$ / $\tau_{u\_predicted}$									
	CF-SWMSTs					CF-SWSSTs				
	Eq. (2)	Eq. (3)	Eq. (4)	Eq. (5)	Eq. (6)	Eq. (2)	Eq. (3)	Eq. (4)	Eq. (5)	Eq. (7)
MS(SS)D1L12A	1.72	1.69	10.19	1.32	0.98	1.04	1.02	6.41	0.80	0.86
MS(SS)D2L12A	1.00	1.18	N/A	0.92	1.21	1.07	1.27	N/A	0.99	0.69
MS(SS)D3L12A	0.87	1.33	N/A	N/A	0.77	1.60	2.45	N/A	N/A	1.09
MS(SS)D2L13A	1.36	1.48	5.76	0.58	1.27	2.71	2.96	11.41	1.16	1.40
MS(SS)D3L13A	1.16	1.53	N/A	0.80	1.05	1.76	2.33	N/A	1.22	0.84
Average	1.22	1.44	7.98	0.91	1.05	1.64	2.00	8.91	1.04	0.98
Stdev	0.33	0.19	3.13	0.31	0.20	0.68	0.83	3.53	0.19	0.28
MS(SS)D1L12B	1.68	1.64	0.93	1.29	1.01	1.17	1.15	0.65	0.90	1.08
MS(SS)D2L12B	0.58	0.69	N/A	0.54	0.73	0.88	1.04	N/A	0.81	0.66
MS(SS)D3L12B	1.42	2.16	N/A	N/A	1.33	1.85	2.82	N/A	N/A	1.63
MS(SS)D2L13B	0.68	0.74	0.28	0.29	0.67	1.43	1.56	0.59	0.61	0.83
MS(SS)D3L13B	0.98	1.30	N/A	0.68	0.94	1.83	2.42	N/A	1.27	1.02
Average	1.07	1.31	0.61	0.70	0.94	1.43	1.80	0.62	0.90	1.05
Stdev	0.47	0.62	0.46	0.42	0.26	0.42	0.79	0.05	0.27	0.37
Average all	1.14	1.38	4.29	0.80	1.00	1.53	1.90	4.76	0.97	1.01
Stdev all	0.39	0.44	4.63	0.36	0.23	0.54	0.77	5.20	0.23	0.31

experimentally for the tested CF-SWSTs were not satisfactorily predicted by the models that were evaluated.

Two of the models that were considered gave zero predictions of bond strength for some of the tested specimens, especially for those with larger D/t ratios. Actual- to-predicted bond strength ratios were not calculated for such cases and are denoted 'N/A' in Table 7 accordingly. Even the model predicted by Lyu and Han (2019) gave acceptable predictions of bond strength only for the CF-SWMSTs but not for the CF-SWSSTs. This indicated the need to have separate expressions for the bond strength prediction of CF-SWSTs distinct to those of CFSTs of other tube types.

$$\tau_u(\text{MPa}) = 0.071 + 4900\left(\frac{t}{D^2}\right) \tag{2}$$

$$\tau_u(\text{MPa}) = 5376.4\left(\frac{t}{D^2}\right) \leq 1.138 \text{ MPa} \tag{3}$$

$$\tau_u(\text{MPa}) = \left[131.227\text{-}1.442\left(\frac{D}{t}\right)\right](0.0067 f_{cu})^{3.84} \tag{4}$$

where f_{cu} is the concrete cube strength in Mpa.

$$\tau_u(\text{MPa}) = 2.314 - 0.0195\left(\frac{D}{t}\right) \tag{5}$$

4.3 Proposed predictive models for bond strength of CF-SWMSTs and CF-SWSSTs

As discussed in Section 4.2, it was found that analytical bond strength models that have previously been proposed did not give satisfactory predictions for the tested CF SWSTs. Consequently, using the experimentally obtained bond strengths, two equations, given in Eqs. (6) and (7), were developed by the authors through regression analysis for the bond strength prediction of CF-SWMSTs and CF-SWSSTs respectively. As can be seen from Fig. 6, since the experimentally obtained bond strength was observed to be strongly dependant on the D/t ratio and to a lesser degree on the concrete strength (f_{cm}), these two parameters were considered when developing Eqs. (6) and (7).

For CF-SWMSTs (f_{cm} in MPa)

$$\tau_u(\text{MPa}) = \left[\frac{1}{5.052 \ln\left(\frac{D}{t}\right) \text{-}19.458}\right] f_{cm}^{-0.11} + 0.078 \tag{6}$$

For CF-SWSSTs (f_{cm} in MPa)

$$\tau_u(\text{MPa}) = \left[\frac{1}{0.324 \ln\left(\frac{D}{t}\right) \text{-}0.905}\right] f_{cm}^{-0.10} \text{-} 0.735 \tag{7}$$

The actual-to-predicted bond strength ratios corresponding to Eqs. (6)-(7) are also tabulated in Table 7. As can be seen from the tabulated values, on average, the predictions of the proposed equations agreed satisfactorily with the experimental values. However, the veracity and robustness of the proposed predictive equations should be verified in the future through additional tests of mild-steel and stainless-steel CF-SWSTs. This is especially so since the developed equations are only strictly valid for the D/t range and f_{cm} values considered for the tests described in this paper. It should be noted that for the development of Eqs. (6)-(7) only the push-out tests conducted on specimens

with the shorter interface length (i.e., L = L1) were used, for reasons discussed previously. It should be noted that Eqs. (6)-(7) are possibly only valid for CF-SWSTs which utilises single-sided SWTs as the bond strength behaviour of SWTs with double-sided welds is unlikely to be the same as those with single-sided welds, as discussed previously.

The bond tests described in this paper did not explicitly consider the effects of concrete shrinkage since a typical normal SCC mix produced by an industry supplier was used for the tested CF-SWSTs. As a result, concrete shrinkage has not been explicitly considered in the developed predictive equations as well. Furthermore, Eqs. (6) and (7) are also only strictly applicable for the prediction of short-term bond strengths since the effects of concrete age was also not considered explicitly in this study. However, as discussed in Section 1, concrete shrinkage and age can have detrimental effects on the bond strength of CFSTs especially in the longer term. Hence, their effects on the push-out bond strength of CF-SWSTs warrant further investigation in the future.

5. Conclusions

Based on the experimental programme that was carried out the following conclusions and recommendations for further work can be made;

- The study showed that the ULS push-out bond strengths of CF-SWMSTs and CF-SWSSTs are either similar to or greater than those of comparable mild-steel and stainless-steel CFSTs of other tube types. This equivalence of bond behaviour provides further evidence that SWTs can be used as direct replacements for their longitudinally welded and seamless counterparts in CFSTs.
- The ULS bond strength showed a decreasing trend with the D/t ratio for both CF-SWMSTs and CF-SWSSTs though no consistent trend could be found for its variation with concrete compressive strength. This behaviour is consistent with the corresponding trends observed for CFSTs of other tube types.
- The push-out bond strength and the form of the load-slip behaviour of CF-SWSTs appear to be similar irrespective of the tube material. This indicates that the inner bead of the spiral weld seam possibly affects the mechanism of push-out resistance, which suggests that SWTs with double-sided welds could have further beneficial effects.
- The fact that, in general, monotonically increasing load-slip behaviour was observed for the tested CF-SWMSTs and CF-SWSSTs indicates that the inner weld bead of a SWT acts as a form of mechanical connector at the steel-concrete interface.
- The experimentally obtained bond strengths appeared to decrease with L/D. The reasons behind this reduction should be further investigated in the future through instrumentation of the steel tube to ascertain how the push-out load is transferred along the length of the specimen.
- The guidelines of AISC-360 were found to provide conservative, yet satisfactorily close predictions of bond strength for both mild steel and stainless-steel CF-SWSTs. This indicated their suitability for bond strength prediction of CF-SWSTs. On the contrary, the bond strength values suggested in AS 2327, AS 5100.6 and Eurocode 4 were significantly non-conservative and warrant reconsideration.
- Based on the test results, equations were developed for estimating the push-out bond strengths of CF-SWMSTs and CF-SWSSTs. The general applicability of these equations to CF-SWSTs needs to be further verified through additional testing in the future.
- It is recommended that the effects of concrete shrinkage and age on the push-out bond strength of CF-SWSTs be investigated in the future.

Acknowledgments

The authors wish to thank James Ballard, Jim Waters, Brad Rose and Michael Pederson for the help they extended towards conducting the experimental programme. The first and second authors also wish to acknowledge that their research work is supported by the Australian Government Research Training Program (RTP) scholarships. The work described in this paper was financially supported by the University of Western Australia.

References

Abendeh, R., Ahmad, H.S. and Hunaiti, Y.M. (2016), "Experimental studies on the behavior of concrete-filled steel tubes incorporating crumb rubber", *J. Constr. Steel Res.*, **122**, 251-260. https://doi.org/10.1016/j.jcsr.2016.03.022

Alfawakhiri, F. (1997), *Behavior of High-strength Concrete-filled Circular Steel Tube Beam-columns*, University of Ottawa Ann Arbor.

Aly, T., Elchalakani, M., Thayalan, P. and Patnaikuni, I. (2010), "Incremental collapse threshold for pushout resistance of circular concrete filled steel tubular columns", *J. Constr. Steel Res.*, **66**(1), 11-18. https://doi.org/10.1016/j.jcsr.2009.08.002

American Institute of Steel Construction (2016), ANSI/AISC 360-16.

Architectural Institute of Japan (AIJ) (2001), Standard for Structural Calculation of Steel Reinforced Concrete Structures.

Chen, B.-C. and Chen, J.-K. (2016), "Experimental studies on shear-bearing capacity of headed stud in concrete-filled steel tube", *Gongcheng Lixue/Engineering Mechanics*, **33**(2), 66-73.

Chen, Z., Xu, J., Xue, J. and Su, Y. (2013), "Push-out test on the interface bond-slip behavior and calculation on bond strength between steel tube and recycled aggregate concrete in RACFST structures", *Tumu Gongcheng Xuebao/China Civil Engineering Journal*, **46**(3), 49-58.

Chen, Y., Feng, R., Shao, Y. and Zhang, X. (2017), "Bond-slip behaviour of concrete-filled stainless steel circular hollow section tubes", *J. Constr. Steel Res.*, **130**, 248-263. https://doi.org/10.1016/j.jcsr.2016.12.012

Ding, Q.-J., Zhou, X.-J., Mou, T.-M., Fan, B.-K. and Yan, Y.-L. (2013), "Bond properties at interface of steel fiber reinforced micro-expansion concrete filled steel tube", *Gongneng Cailiao/Journal of Functional Materials*, **44**(6), 809-813.

EN 1994-1-1:2004 (2004), Eurocode 4: Design of composite steel

and concrete structures, Part 1.1, General rules and rules for buildings.

Fu, Z.Q., Ge, H.B., Ji, B.H. and Chen, J.J. (2018), "Interface bond behaviour between circular steel tube and lightweight aggregate concrete", *Adv. Steel Constr*., **14**(3), 424-437.

Grzeszykowski, B., Szadkowska, M. and Szmigiera, E. (2017), "Analysis of stress in steel and concrete in CFST push-out test samples", *Civil Environ. Eng. Reports*, **26**(3), 145-159.

Guan, M., Lai, Z., Xiao, Q., Du, H. and Zhang, K. (2019), "Bond behavior of concrete-filled steel tube columns using manufactured sand (MS-CFT)", *Eng. Struct*., **187**, 199-208. https://doi.org/10.1016/j.engstruct.2019.02.054

Gunawardena, Y. and Aslani, F. (2018), "Behaviour and design of concrete-filled mild-steel spiral welded tube short columns under eccentric axial compression loading", *J. Constr. Steel Res*., **151**, 146-173. https://doi.org/10.1016/j.jcsr.2018.09.018

Gunawardena, Y. and Aslani, F. (2019a), "Behaviour and design of concrete-filled spiral-welded stainless-steel tube short columns under concentric and eccentric axial compression loading", *J. Constr. Steel Res*., **158**, 522-546. https://doi.org/10.1016/j.jcsr.2019.04.013

Gunawardena, Y. and Aslani, F. (2019b), "Concrete-filled spiral-welded stainless-steel tube long columns under concentric and eccentric axial compression loading", *J. Constr. Steel Res*., **161**, 201-226. https://doi.org/10.1016/j.jcsr.2019.07.006

Gunawardena, Y., Aslani, F. and Uy. B. (2019), "Concrete-filled mild-steel spiral-welded tube long columns under eccentric axial compression loading", *J. Constr. Steel Res*., **159**, 341-363.

Kang, X.-L., Cheng, Y.-F., Tu, Y. and Xue, J.-Y. (2010), "Experimental study and numerical analysis of bond-slip performance for concrete filled steel tube", *Gongcheng Lixue/Engineering Mechanics*, **27**(9), 102-106.

Ke, X., Sun, H., Chen, Z., Su, Y. and Ying, W. (2015), "Interface mechanical behavior test and bond strength calculation of high-strength concrete filled circular steel tube", *Jianzhu Jiegou Xuebao/Journal of Building Structures*, **36**, 401-406.

Knoop, F.M. and Sommer, B. (2004), *Manufacturing and use of spiral welded pipes for high pressure service - State of the art*, American Society of Mechanical Engineers, Calgary, Alta, Canada.

Kyriakides, S. and Corona, E. (2007), *Mechanics of Offshore Pipelines*, Elsevier Ltd.

Lehman, D., Roeder, C. and Stephens, M.T. (2018), *Concrete-filled tube bridges for accelerated bridge construction*, University of Washington.

Lu, Y., Liu, Z., Li, S. and Li, N. (2018a), "Bond behavior of steel fibers reinforced self-stressing and self-compacting concrete filled steel tube columns", *Constr. Build. Mater*., **158**, 894-909. https://doi.org/10.1016/j.conbuildmat.2017.10.085

Lu, Y., Liu, Z., Li, S. and Tang, W. (2018b), "Bond behavior of steel-fiber-reinforced self-stressing and self-compacting concrete-filled steel tube columns for a period of 2.5 years", *Constr. Build. Materi*., **167**, 33-43. https://doi.org/10.1016/j.conbuildmat.2018.01.144

Lyu, W.-Q. and Han, L.-H. (2019), "Investigation on bond strength between recycled aggregate concrete (RAC) and steel tube in RAC-filled steel tubes", *J. Constr. Steel Res*., **155**, 438-459.

Morino, S. and Tsuda, K. (2003), "Design and construction of concrete-filled steel tube column system in Japan", *Earthq. Eng. Eng. Seismol*., **4**(1), 51-73.

Radhika, K.S. and Baskar, K. (2012), "Bond stress characteristics on circular concrete filled steel tubular columns using mineral admixture metakaoline", *Int. J. Civil Struct. Eng*., **3**(1), 1-8.

Radhika, K.S. and Baskar, K. (2013), "Bond stress characteristics on circular concrete filled steel tubular columns using mineral admixture silica fume", *Int. J. Earth Sci. Eng*., **6**(1), 170-177.

Rasmussen, K.J.R. (2003), "Full-range stress–strain curves for stainless steel alloys", *J. Constr. Steel Res*., **59**(1), 47-61. https://doi.org/10.1016/S0143-974X(02)00018-4

Roeder, C.W., Cameron, B. and Brown, C.M. (1999), "Composite action in concrete filled tubes", *J. Struct. Eng*., **125**(5), 477-484. https://doi.org/10.1061/(ASCE)0733-9445(1999)125:5(477)

Roeder, C.W., Lehman, D.E. and Thody, R. (2009), "Composite action in CFT components and connections", *Eng. J*., **46**(4), 229-242.

ROLADUCT Spiral Tubing Group (2017), *Spiral Welded Tube, Pipe & Fittings: Product Information*.

Sadowski, A.J., Van Es, S.H.J., Reinke, T., Michael Rotter, J., Nol Gresnigt, A.M. and Ummenhofer, T. (2015), "Harmonic analysis of measured initial geometric imperfections in large spiral welded carbon steel tubes", *Eng. Struct*., **85**, 234-248. https://doi.org/10.1016/j.engstruct.2014.12.033

Shakir-Khalil, H. (1993), "Pushout strength of concrete-filled steel hollow section tubes", *Struct. Engineer*, **71**(13).

Standards Australia (2007), AS/NZS 1391-2007.

Standards Australia (2017a), AS/NZS 2327:2017.

Standards Australia (2017b), AS/NZS 5100.6:2017.

Tao, Z., Han, L.-H. and Uy, B. (2012), "Behaviour of concrete-filled stainless steel tubular columns at ambient and elevated temperatures", Qingdao, China.

Tao, Z., Song, T.-Y., Uy, B. and Han, L.-H. (2016), "Bond behavior in concrete-filled steel tubes", *J. Constr. Steel Res*., **120**, 81-93. https://doi.org/10.1016/j.jcsr.2015.12.030

Tremayne, H., Mahin, S.A., Monterrosa, J.A., Dean, S., Fong, C., Jachens, E.R., Lam, D., Minner, M., Pavicic, J. and Rodriguez, L. (2013), *Earthquake Engineering for Resilient Communities: 2013 PEER Internship Porgram Research Report Collection*, Pacific earthquake engineering research center.

Virdi, K.S. and Dowling, P.J. (1980), "Bond strength in concrete filled steel tubes", *IABSE Periodica*, **33**(80), 15.

Xu, C., Chengkui, H., Decheng, J. and Yuancheng, S. (2009), "Push-out test of pre-stressing concrete filled circular steel tube columns by means of expansive cement", *Constr. Build. Mater*., **23**(1), 491-497. https://doi.org/10.1016/j.conbuildmat.2007.10.021

Xu, J., Chen, Z., Xue, J. and Su, Y. (2013), "Failure mechanism of interface bond behavior between circular steel tube and recycled aggregate concrete by push-out test", *Jianzhu Jiegou Xuebao/Journal of Building Structures*, **34**(7), 148-157.

Xu, K., Bi, L. and Chen, M. (2015), "Experimental study on bond stress-slip constitutive relationship for CFST", *Jianzhu Jiegou Xuebao/Journal of Building Structures*, **36**, 407-412.

Yan, Z., An, M., Wu, P., Li, J. and Zhang, L. (2009), "Experimental study of the bond strength at the interface of reactive powder concrete-filled steel tube columns", *Zhongguo Tiedao Kexue/China Railway Science*, **30**(6), 7-11.

Yin, X. and Lu, X. (2010), "Study on push-out test and bond stress-slip relationship of circular concrete filled steel tube", *Steel Compos. Struct., Int. J*., **10**(4), 317-329. https://doi.org/10.12989/scs.2010.10.4.317

Yuan, X. and Chen, X. (2018), "Effect analysis of expansion agent on interfacial bond behavior of concrete filled steel tubular", *Chem. Eng. Transact*., **66**, 1165-1170. https://doi.org/10.3303/CET1866195

Zhang, J., Denavit, M.D., Hajjar, J.F. and Lu, X. (2012), "Bond behavior of concrete-filled steel tube (CFT) structures", *Eng. J*., **49**(4), 169-185.

CC

Nomenclature

CFST	Concrete-filled steel tube
CFSST	Concrete-filled stainless-steel tube
CF-SWMST	Concrete-filled spiral-welded mild-steel tube
CF-SWST	Concrete-filled spiral-welded steel tube
CF-SWSST	Concrete-filled spiral-welded stainless-steel tube
CS	Carbon steel
D	Outside diameter of steel tube
EA	Expansive additives
E_0	Initial elastic modulus of stainless-steel
E_s	Elastic modulus of mild steel
f'_c	Concrete strength grade
f_{cm}	Mean concrete cylinder compressive strength
f_y	Yield strength of mild steel
$f_{0.2\%}$	0.2% proof stress
HSC	High strength concrete
MS	Mild steel
L	Length of steel-concrete interface
LAC	Lightweight aggregate concrete
LSA	Low shrinkage additives
LWT	Longitudinally welded tube
n	Non-linearity ratio
P	Applied test load
$P_{push\text{-}out}$	Applied load corresponding to ULS bond strength
RAC	Recycled aggregate concrete
RPC	Reactive powder concrete
RuC	Rubberised concrete
t	Wall thickness of tube
t_{age}	Age of concrete
s	Interface slip
SF(R)	Steel fibre (reinforced)
SCC	Self-compacting concrete
SS	Stainless-steel
SS-SWT	Stainless-steel spiral-welded tube
SWT	Spiral welded tube
ULS	Ultimate limit state
ε_{bond}	Bond strain (= s/L)
τ	Average bond stress (uniform bond stress acting over interface area)
τ_{bond}, τ_u	Ultimate limit state bond strength (average bond strength)
$\tau_{u\_experimental}$	Experimentally obtained ULS bond strength
$\tau_{u\_predicted}$	Predicted ULS bond strength